applied sciences

MDPI

Article

A Novel Clamping–Cooling System for the Off-Axis Machining of Hydrophobic Micro-Optics

Wei Wang [1,*], Oltmann Riemer [1,2], Kai Rickens [1], Timo Eppig [3,4], Alexander Baum [3] and Bernhard Karpuschewski [1,2]

[1] Laboratory for Precision Machining (LFM), Leibniz Institute for Materials Engineering (IWT), Badgasteiner Str. 3, 28359 Bremen, Germany; riemer@iwt.uni-bremen.de (O.R.); rickens@iwt.uni-bremen.de (K.R.); karpuschewski@iwt-bremen.de (B.K.)
[2] MAPEX Center for Materials and Processes, University of Bremen, Bibliothek Str. 1, 28359 Bremen, Germany
[3] Advanced Medical Implant Consulting (AMIPLANT GmbH), Haidling 1, 91220 Schnaittach, Germany; timo.eppig@mx.uni-saarland.de (T.E.); alexander.baum@amiplant.com (A.B.)
[4] Institute of Experimental Ophthalmology, Saarland University, Kirrberger Straße 100, 66421 Homburg/Saar, Germany
* Correspondence: wang@iwt-bremen.de; Tel.: +49-421-218-51162

Featured Application

The proposed clamping–cooling system provides a stable 0.3 K thermal regulation solution for the scalable, off-axis ultra-precision machining of temperature-sensitive polymers, enabling nanoscale surface integrity and nanometric surface finish. Its primary application is the manufacturing of medical devices, specifically hydrophobic intraocular lenses (IOLs). Beyond medical manufacturing, the system's adaptable design makes it highly relevant to industries that require scalable production of complex micro-optical components, including telecommunications, automotive LIDAR, augmented/virtual reality systems, and photonic devices.

Abstract

The ultra-precision machining of micro-optics from low glass transition temperature (T_g) hydrophobic polymers is frequently compromised by thermal instability and kinematic constraints imposed by on-axis turning. To address these challenges, this study presents a novel clamping–cooling system engineered for the off-axis diamond turning of low-T_g polymers. The design integrates vacuum clamping for workpiece stabilization with an embedded microchannel network for efficient thermal management. Strategic material selection effectively balances thermal insulation with mechanical stability. Performance evaluations demonstrated robust thermal regulation: lens blank surface temperatures stabilized at 6 °C during stationary testing, and the system was able to drop below 0 °C under maximum cooling targets. This strict thermal control enabled achieving nanometer surface roughness. Ultimately, this modular system facilitates the scalable, simultaneous production of high-quality, polishing-free intraocular lenses (IOLs), advancing manufacturing capabilities for complex precision optics.

Keywords: clamping technology; ultra-precision; diamond turning; polymer; cooling

Check for updates

Academic Editor: Alexandre Carvalho

Received: 16 January 2026
Revised: 6 April 2026
Accepted: 8 April 2026
Published: 10 April 2026

Copyright: © 2026 by the authors. Licensee MDPI, Basel, Switzerland. This article is an open access article distributed under the terms and conditions of the Creative Commons Attribution (CC BY) license.

1. Introduction

Micro-optics is a specialized subfield within optics dedicated to the design and implementation of optical components with microscale features, typically measuring less than a

few millimeters and requiring surface tolerances at the nanometer scale. Core micro-optical elements include micro-lenses, micro-prisms, diffractive optical elements (DOEs), and micro-mirrors, which are essential for the miniaturization and enhancement of optical systems in high-precision applications. Micro-optics are critical in a range of sectors: in telecommunications, enhancing fiber-optic networks through efficient light manipulation; in consumer electronics, enabling compact, high-resolution cameras and projectors; and in healthcare, improving imaging quality in endoscopic and diagnostic devices. Further applications encompass LIDAR technology for autonomous vehicles, 3D sensing for facial recognition, and augmented/virtual reality systems, where micro-optics facilitate compact, high-resolution displays. Additionally, emerging domains such as quantum and photonic computing employ micro-optics for precise photon control, underscoring their growing role in advanced technological fields.

As optical devices continue to miniaturize, ensuring fabrication precision has become increasingly challenging, with even minimal deviations significantly affecting optical performance. To meet these stringent demands, clamping systems are critical for maintaining precise, stable positioning of micro-optical components during key production stages, including cutting, grinding, polishing, and coating. Clamping systems used in micro-optics manufacturing must satisfy rigorous standards for positioning accuracy, minimal deformation, and thermal stability. Unlike larger optical components, micro-optical elements are particularly sensitive to mechanical stress and thermal fluctuations. Consequently, an effective clamping system must deliver high stability and minimal contact pressure to prevent deformation or misalignment, which could degrade optical properties.

Furthermore, clamping systems must be compatible with high-precision machining and assembly platforms, often requiring operation within cleanroom environments maintained at a stable ambient temperature (20 °C) to mitigate contamination and thermal expansion. In the context of micro-optics, the pursuit of ultra-precision machining is quantitatively defined by the capability to achieve nanoscale surface roughness and sub-micrometer form accuracy [1–3]. Meeting these requirements is particularly challenging when machining is only feasible at suppressed temperatures; this necessitates a clamping system that can thermally decouple the machine tool—which must remain at a constant ambient temperature for structural stability—from the workpiece, which requires a cryogenic or low-temperature environment.

To date, the mechanical micromachining of soft polymers with cryogenic assistance has not been fully established [4]. A practical example of such a scenario is the fabrication of low T_g hydrophobic IOLs [5], where precise temperature control below the T_g is critical to maintaining optical quality and performance. The precision and surface quality of these lenses are paramount, as they directly influence the visual outcome and patient satisfaction [6].

IOLs are critical optical devices surgically implanted to replace the natural crystalline lens in cataract patients, restoring vision and preventing blindness, as illustrated in Figure 1. The requirement for such cataract surgery arises when the opacification significantly impedes vision. There are about 3.7 million cases per year in the USA, 7 million in Europe, and 20 million cataract surgeries conducted annually all over the world [7].

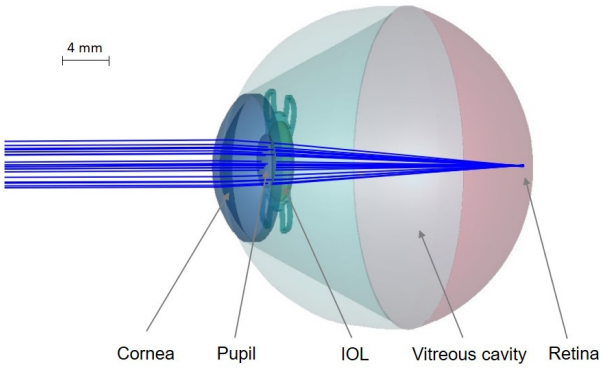

Figure 1. The structure of the eyes and the position of an IOL in a human eye.

The global IOL market is estimated at USD 4.6 billion in 2023 and is projected to reach USD 6.8 billion by 2030, growing at a compound annual growth rate (CAGR) of 5.7% from 2023 to 2030 [8]. Despite high market demand, production capacity, particularly for customized lenses, remains constrained, while standard IOLs are mass-produced by molding processes. Customized lenses, however, have the potential to correct for individual aberrations, thereby improving visual outcomes not only in highly aberrated eyes [9]. On-axis diamond turning is the standard method for manufacturing customized IOLs, directly shaping blanks to optical quality [6]. Studies on machining parameters for polymethyl methacrylate (PMMA) [10,11] and polycarbonate (PC) [12,13] demonstrate that single-point diamond turning (SPDT) reduces surface roughness and profile error. However, fabricating a single freeform optic lens in this way takes up to 30 min, significantly limiting production scalability.

To address the challenge in production capacity, Wang et al. [14] proposed a potential solution to enhance the productivity of hydrophobic IOLs through parallelized processing using Off-Axis Fast-Tool-Servo (FTS) diamond turning. This innovative method highlights the necessity of an off-axis clamping system equipped with in-process cooling, ensuring precision and stability throughout the manufacturing process. Research indicates that no such clamping system currently exists on the market, necessitating the development of a tailored solution.

This paper presents an in-house-designed clamping–cooling system specifically developed to address this technological gap. The work begins with an overview of the manufacturing process for customized IOLs, followed by an introduction to the standard clamping technology used in IOL production: the mandrel, or quill. The design process is comprehensively detailed, covering the underlying design principles, the selection of optimal solutions for key subsystem functions—off-axis machining, clamping, and cooling technologies—and the material selection for each component. Finally, a stationary performance test confirms that the developed clamping–cooling system meets the stringent thermal management requirements for off-axis FTS diamond turning of low-T_g hydrophobic IOLs and other micro-optics.

2. Manufacturing of Customized IOLs

Precision molding is preferred in the industrial production of IOLs due to its high efficiency and excellent repeatability. However, it is primarily suitable for mass production because ultra-precision mold machining is both time-consuming and costly. For the manufacturing of customized IOLs, diamond turning is commonly employed, enabling direct machining of the optical surface onto the IOL substrate [6]. In this case, the machining process can be divided into two stages: diamond turning of the optic part and diamond milling of the haptic part.

IOL manufacturing is subject to rigorous quality protocols, primarily governed by ISO 11979-2 [15] and ISO 11979-3 [16]. To ensure optimal optical performance and mechanical stability, dimensional tolerances for the clear optic diameter and overall diameter must be strictly constrained, typically within ± 0.15 mm and ± 0.20 mm, respectively, in accordance with the permissible deviations defined in ISO 11979-3. Furthermore, surface integrity is a critical determinant of biocompatibility and of minimizing light scattering. To comply with the Modulation Transfer Function (MTF) requirements specified in ISO 11979-2 (e.g., MTF $\geq$ 0.43 at 100 lp/mm), the machined surfaces must achieve nanoscale roughness. Characterized by the arithmetical mean height of the scale-limited surface (Sa) as defined in ISO 25178-2 [17], this roughness is typically required to be Sa < 20 nm. Such precision is essential to mitigate the risk of posterior capsule opacification and ensure superior visual outcomes.

The specimens utilized in this study were fabricated from SHi49 (Contamac Ltd., Saffron Walden, UK), a high-purity, hydrophobic acrylic polymer used in IOLs. SHi49 is characterized by a refractive index of 1.49, a Shore A hardness of 60 $\pm$ 10, and a low equilibrium water content (<1%). Notably, the material exhibits a T_g of approximately 10 °C, which is significantly below ambient room temperature.

The first step involves machining the optic part—both the front and rear sides—which is responsible for vision correction. This process is typically performed using ultra-precision diamond turning under computer numerical control (CNC). The lens blank, measuring 16 mm in diameter as shown in Figure 2a, is mounted securely on a rotating spindle. A diamond-tipped tool then removes material with sub-micron accuracy, enabling the generation of complex surface geometries such as aspheric, toric, and multifocal designs. Critical machining parameters, including spindle speed, feed rate, and cutting depth, are precisely controlled to ensure exceptional surface quality and optical performance. After completing the front side machining (as shown in Figure 2b), the lens is repositioned with high accuracy for machining of the rear side, ensuring positional precision and geometric consistency throughout the process.

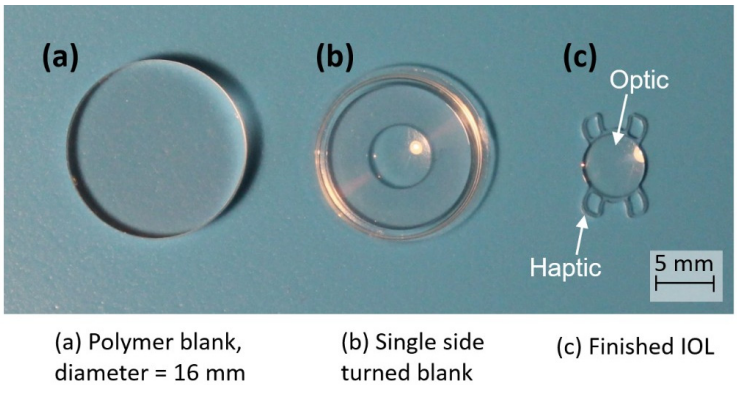

Figure 2. Machining procedure of customized IOL by diamond turning.

After the diamond turning of the rear side is completed, the next step is diamond milling of the haptic elements, which play a crucial role in ensuring the stable fixation of the IOL within the eye's capsular bag. The haptics are designed with precise dimensions to guarantee stability, centering, and long-term biocompatibility. The haptic geometry varies depending on the specific application and machining requirements. Common designs include C-loop, plate-haptic, and modified haptics with flexible arms to improve adaptability during implantation. A finished IOL with four-loop haptics is shown in Figure 2c.

3. Standard IOL Clamping Technology

For the implementation of the different machining processes, i.e., diamond machining of the front and back sides as well as milling of the haptic, two different mandrel/quill-type on-axis clamping devices are required for the standard manufacturing sequence. Design and application of these devices are depicted in detail in the following.

3.1. Design of On-Axis Blank Holders

Based on the process requirements, two different holders are used to clamp the blanks, as shown in Figure 3. A common base element is used for both holders, while the head element is adapted for machining the front and rear sides of the blank, respectively.

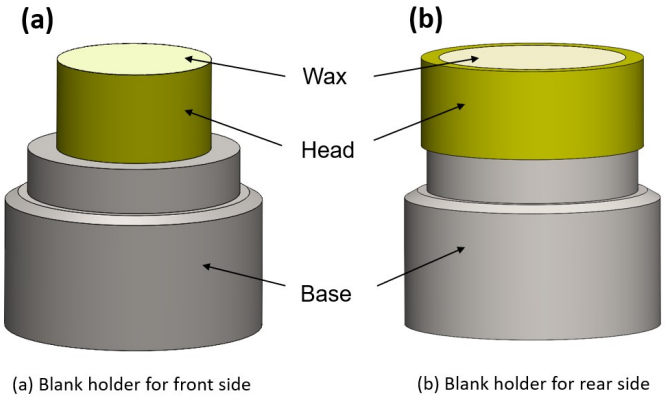

Figure 3. Schematic design and structure of holders for the clamping of IOL blanks for the front and rear side machining.

3.2. Manufacturing Sequence Using On-Axis Clamping

The overall manufacturing sequence for an individual IOL is subdivided into seven production steps, as shown in Figure 4.

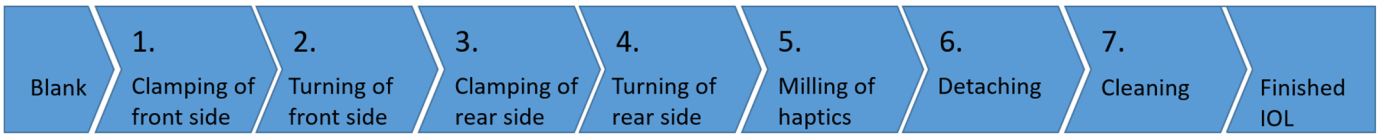

Figure 4. Machining steps for the production of customized IOLs.

Firstly, a polymer blank is waxed onto a flat blank holder for the machining of the IOL front side. To begin, the clamping device is primarily checked for cleanliness, then heated, and finally, an accurately defined amount of wax is applied at the center of the clamping surface. Subsequently, a blank is positioned in the upper part of the blocking station (clamping chuck), as shown in Figure 5, and the hot blank holder with liquid wax is positioned below on the base of the blocking station. The chuck is lowered until the blank rests on the molten wax, and the entire assembly is cooled until the wax is completely solidified. After opening the chuck, the blank holder can be removed for the next machining step.

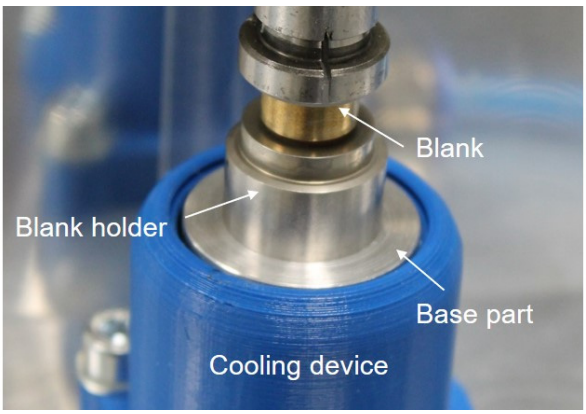

Figure 5. Blocking station for joining IOL blanks to the blank holder.

Next, the blank holder is attached to the clamping system of an ultra-precision lathe, and the optical front surface of the IOL and the flat front side for the haptic are generated by diamond turning (Figure 6). The component is briefly checked on-machine, and the blank holder is removed from the machine tool's clamping system for further processing.

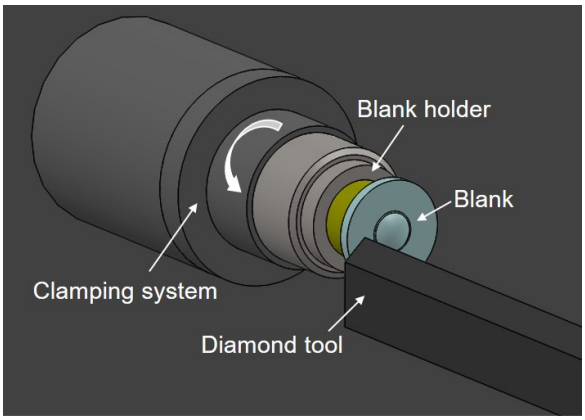

Figure 6. Diamond turning of the front side of an IOL.

Similar to the first manufacturing step, the blank holder for the rear side is then heated, waxed, and placed in the base of the blocking station. Likewise, the blank holder with the machined front side is positioned in the upper chuck of the blocking station. After cooling, the blank holder for the front side is detached from the assembly, and the one-sided machined polymer blank is transferred to the second blank holder.

For machining the rear side of the IOL, the blank holder is mounted on the ultra-precision lathe, and the entire back side is diamond-turned, i.e., the optical and haptic surfaces. Finally, the IOL contour is milled and the IOL detached from the blank holder. Subsequently, blank holders require cleaning for the next production cycle, while the IOL is cleaned and then handed over to inspection and packaging.

3.3. Comparison of On- and Off-Axis Machining

While on-axis turning—where the geometric center of the workpiece coincides with the spindle's rotational axis—is a common approach for fabricating customized IOLs, it possesses an inherent kinematic limitation regarding surface integrity at the optical apex. This constraint arises from the fundamental relationship governing the local cutting velocity (v_c) in any turning process, as defined in Equation (1):

$$v_c = \pi \cdot D \cdot n \quad (1)$$

where D represents the local cutting diameter, and n denotes the spindle rotational speed. In an on-axis configuration, the diameter D approaches zero as the tool moves toward the center of the lens. This mathematically dictates that the cutting velocity v_c must also drop to zero, regardless of the programmed spindle speed.

Within this zero-velocity zone, the material removal mechanism transitions from efficient shearing to a combination of stagnant compression and uncontrolled plastic deformation. This ineffective cutting results in a prominent central material artifact [18], as demonstrated by the interferometric characterization in Figure 7, obtained using a NewView white-light interferometer (Zygo Corporation, Middlefield, CT, USA) equipped with a 20× Mirau objective.

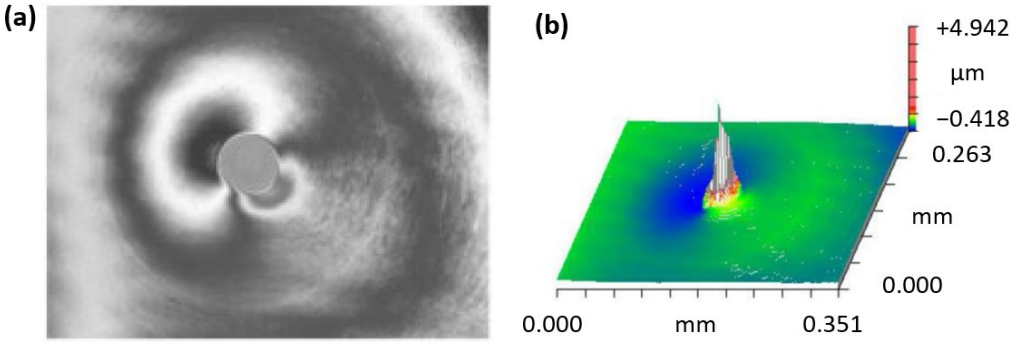

Figure 7. Visualization of central artifact from on-axis machining through Interferometry: (**a**) Raw Intensity Fringes and (**b**) 3D Surface Reconstruction.

Figure 7a shows the raw interference intensity map, with concentric fringes representing the phase-shift data. Figure 7b provides a three-dimensional isometric oblique plot of the reconstructed topographic data. This map reveals a localized, high-aspect-ratio vertical "spike" at the center of the otherwise smooth surface, indicating that residual material protrudes significantly above the nominal design profile. Such artifacts are detrimental to the lens's optical performance and necessitate post-polishing. However, post-polishing processes can compromise the sub-micron form accuracy of customized freeform surfaces and introduce additional manufacturing costs.

In contrast, off-axis machining circumvents this kinematic singularity by positioning the IOL substrate at a defined radial offset (R_{offset}). This configuration ensures that a sufficient cutting velocity is maintained with a proper R_{offset}, also at the geometric center of the lens, as defined in Equation (2):

$$v_c = \pi \cdot 2 \cdot R_{offset} \cdot n \quad (2)$$

This kinematic advantage effectively suppresses the formation of central artifacts, enabling the production of "polishing-free" optical surfaces across the entire aperture.

Beyond these qualitative advantages, the off-axis configuration offers significant gains in manufacturing throughput. While traditional on-axis processes limit machining to a single lens per cycle, off-axis machining enables parallelized processing. By mounting multiple substrates at the same radial offset, the effective machining time per lens is substantially reduced. Furthermore, eliminating mandatory post-polishing—required to remediate the aforementioned central artifacts—preserves sub-micron form accuracy while minimizing labor and overhead costs, offering a more robust solution for high-volume production.

4. Design Process for a Novel Off-Axis Clamping–Cooling System

The standard mandrel/quell clamping technology described in Section 3 features on-axis clamping with wax and is widely used in the production of IOLs from PMMA and hydrophilic polymers, where deep cooling is not required. However, it proves infeasible for low-T_g hydrophobic polymers, as wax loses effectiveness at low temperatures. To overcome this limitation, the proposed novel clamping–cooling system enables off-axis machining with in-process temperature control, ensuring stable performance under cooling conditions.

From the perspectives of machining, cooling, and clamping technologies, various alternatives are evaluated, leading to the development of a schematic design for a novel clamping–cooling system tailored for ultra-precision off-axis machining of hydrophobic IOLs.

4.1. Machining Process—Off-Axis Turning

The distinction between on-axis and off-axis machining lies in the alignment of the spindle axis relative to the workpiece axis, as mentioned in Section 3. In on-axis machining, the spindle axis aligns with the rotational axis of the workpiece, offering high precision, repeatability, and cost efficiency. In contrast, off-axis machining positions the workpiece distant from the spindle axis, enabling the simultaneous machining of multiple surfaces. This configuration provides greater flexibility for producing complex micro-optical components and has the potential to increase productivity.

In this study, the number of lenses is set to three to evaluate productivity gains. The lens positions are arranged as shown in Figure 8, corresponding to the computer-aided manufacturing (CAM) programming layout. They form a rotationally symmetric distribution on the clamping device with an included angle of 120°. The turning radius, defined as the distance between the center of each lens and the spindle axis, is set to 115 mm.

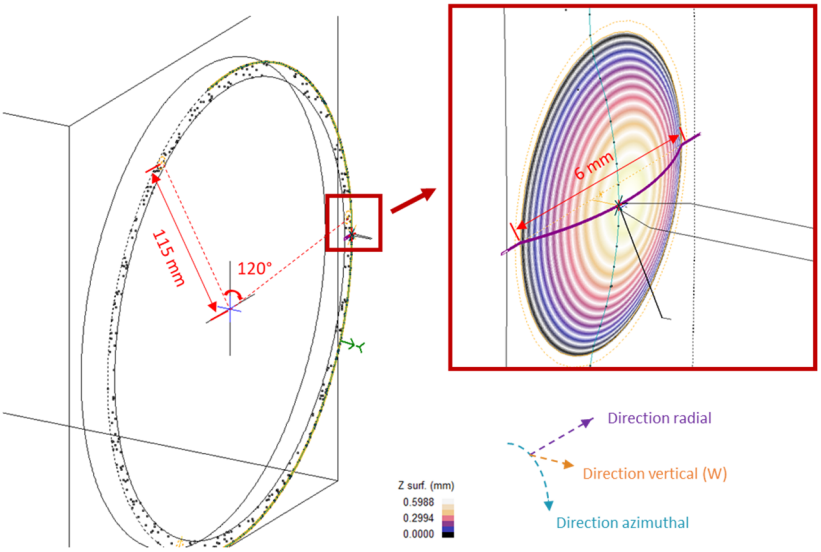

Figure 8. CAM-simulated tool path, IOLs with cutting path area (r = 115 mm, blue) and lens geometry (+20D PMMA, d = 6 mm, colored).

4.2. Cooling—Microchannel Cooling System

Unlike on-axis machining, off-axis machining of multiple IOLs simultaneously is significantly more time-consuming, requiring sustained cooling to maintain low temperatures and ensure material integrity. The available cooling technologies are evaluated based on various factors, including cooling capacity and precision, temperature control stability, material compatibility, and cost-effectiveness. Table 1 presents a detailed evaluation,

highlighting the advantages and challenges of each cooling system in the context of their feasibility for IOL manufacturing.

Table 1. Analysis of cooling technologies and their feasibility for IOL machining.

Cooling Technology	Advantages	Challenges	Feasibility and Cost Analysis
Cryogenic Cooling (LN_2/CO_2) [19]	– Ultra-low temperatures – Rapid cooling – Precise temperature control	– High setup and operational costs – Safety requirements – Risk of thermal shock	Suitable if stringent temperature control is applied. Effective in specific stages, but the risk of thermal damage limits its widespread use. Low initial setup cost, but high recurring maintenance and disposal costs.
Minimum Quantity Lubrication (MQL) with Coolants [20]	– Minimal coolant use – Reduced contamination – Cost-effective	– Insufficient cooling for low-T_g materials – Compatibility issue between Oil-based coolants and hydrophobic polymers	Limited cooling capacity and material compatibility concerns make it unsuitable for heat-sensitive and delicate IOL manufacturing. Moderate initial cost and very low operational cost.
Phase Change Materials (PCMs) [21]	– Passive, stable cooling – Low thermal stress – Mold compatibility	– Slow temperature response – Limited temperature range	Effective in passive applications, such as mold cooling, but unsuitable for rapid, high-precision cooling in IOL turning processes. Complex to integrate PCMs into a rotating chuck or spindle, leading to high cost.
Microchannel Cooling System [22,23]	– Precise cooling – Implementability in off-axis turning – Good temperature gradient control	– Complex design – High setup cost – Potential contamination risks due to coolant leakage	Highly suitable due to precise temperature control and adaptability to complex IOL shapes, ensuring optimal polymer integrity. Moderate initiation cost to create channels within the clamping system and low recurring cost.
Peltier (Thermoelectric) Cooling [24]	– Ultra-precise, localized cooling – Solid-state system, no moving parts – Reduced risk of contamination	– Limited cooling capacity – Low efficiency with cooling load	Niche Feasibility. Excellent for static temperature control, but struggles to dissipate the high heat flux generated during high-speed diamond turning compared to fluid-based microchannels. Relative high cost per watt of cooling.
Conformal Cooling (3D-Printed Cooling Channels) [25]	– Customizable channels for precise mold fitting – Uniform temperature distribution – Homogeneous cooling for complex shape	– High initial costs – Limited to mold-based processes	Suitable for mold-based IOL production, providing consistent cooling that minimizes internal stresses and defects in lenses, while not feasible for the turning process.
Vortex Tube [26]	– Cost-effective – Simple – No refrigerants needed	– Limited precision and temperature control – Insufficient cooling for low-T_g polymers	Inadequate for IOL manufacturing due to the lack of control and insufficient cooling precision. Better suited for less sensitive applications. Low cost.
Laser-Assisted [27]	– Extreme control – Nanoscale precision	– Extremely high cost and complexity – Limited scalability and throughput for industrial applications	Incompatible for IOL production. Since IOL polymers are already too soft, this would likely cause material degradation rather than precision.

Cryogenic cooling, such as liquid nitrogen, provides ultra-low temperatures but poses risks of thermal shock and high operational costs, making it less suitable for precision applications. Minimum Quantity Lubrication (MQL) offers economical cooling with minimal contamination, but its limited cooling capacity is inadequate for low-T_g materials in

high-precision contexts. Phase Change Materials (PCMs) provide stable, passive cooling, yet their slow response to temperature changes limits their effectiveness in dynamic machining environments. Thermoelectric (Peltier) cooling provides precise, localized cooling but lacks the necessary capacity for the full cooling demands in IOL machining. Conformal cooling, using 3D-printed channels that match mold geometry, achieves uniform cooling in mold-based applications, but its inflexibility in material selection limits its ability to prevent heat transfer—a crucial factor in ultra-precision machine tools. Vortex tube cooling, while simple and cost-effective, struggles with the trade-off between achievable low temperature and required gas volume, making it unsuitable for stable off-axis clamping system cooling. Microchannel cooling is the most viable solution in this case, offering precise, even distributed temperature control through coolant flow in embedded microchannels. When coupled with a refrigeration circulation thermostat, microchannel cooling provides enhanced power and stability, ensuring consistent thermal management that protects the integrity of low-T_g polymers and surpasses simpler methods in both precision and cooling capacity for ultra-precision IOL production.

4.3. Clamping—Vacuum

Selecting an optimal clamping technology is crucial in micro-optics machining to ensure lens precision, minimize deformation, and prevent surface contamination. Evaluation criteria for clamping feasibility include surface integrity, precision stability, material compatibility, and maintenance demands, each addressing the unique requirements of medical-grade manufacturing. Various clamping systems are evaluated based on their capacity to provide secure, non-invasive, and precise holding. An evaluation of the advantages and challenges of each is given in Table 2.

The mandrel/quill from Section 3 is an example of wax clamping. The primary advantage of this technique is its simplicity and adaptability to complex geometry. However, wax clamping has limitations, particularly in terms of thermal stability, as it loses effectiveness at low temperatures, which prevents its application in low T_g polymers. Additionally, a post-processing step is required to remove any residual wax contamination from the final product, which can introduce additional complexity and time to the manufacturing process. Cryogenic cooling-assisted ice clamping is another promising method for manufacturing hydrophobic IOLs, as it provides a uniformly distributed holding force by freezing water while simultaneously meeting the cooling requirement. However, for materials with high water affinity, such as hydrophilic polymers, this method poses the risk of water exposure, which could affect material integrity. Additionally, cryogenic cooling-assisted ice clamping is currently limited to fixed holding, and further developments are needed to ensure its effectiveness during the turning process, where dynamic clamping is required.

Compared to more complex systems, such as hydrostatic and compliant fixturing—which provide gentle holding and high adaptability but require intensive maintenance and setup—vacuum clamping offers a simpler and highly effective solution. It delivers uniform, non-contact pressure that securely holds lenses without a high risk of surface damage, making it particularly suitable for delicate optical components. The simplicity and adaptability of vacuum clamping also facilitate its seamless integration into automated production lines, enabling consistent, high-volume, and efficient output with minimal intervention. Other possibilities, such as electromagnetic, hydrostatic, piezoelectric, and compliant clamping, are also evaluated in Table 2 and are not considered due to their limitations in terms of material feasibility, cost, and performance.

Table 2. Analysis of clamping technologies and their feasibility for IOL machining.

Clamping Technology	Advantages	Challenges	Feasibility and Cost Analysis
Wax [28]	– Uniform and stress-free – Suitable for most materials – Adaptability to complex geometry	– High cleaning requirement – Disability at low temperature	Suitable for materials without cooling requirements. Low material cost, but high recurring labor costs due to heating, applying, cooling, and later removing the wax added.
Cryogenic cooling assisted ice [29]	– Uniform and stress-free – No post-processing needed with effective water management	– Material limitation for hydrophilic polymers – Not adaptable for the turning process	Feasible for non-hydrophilic polymer milling, yet not for the turning process. High setup and low operational cost.
Mechanical Vice [30]	– Simple implementation – High stability	– High risk of applying excessive force – Ununiformed force distribution	Not feasible for micro-components like IOLs due to the high risk of inducing localized stress and distorting thin optical polymers. Low cost.
Vacuum [31]	– Uniform pressure distribution – No mechanical force – Stable hold for flat or mildly curved surfaces.	– Surface limitations in Curvature radius – Risk of deformation – Complex setup for contours	Excellent for applying a uniform holding force without marring the surface. Feasible for flat or gently curved lenses in precision processes. Requires custom tooling for curved lenses. Moderate cost.
Electromagnetic [32]	– Fast clamping/unclamping – No mechanical interference	– Material limitations – High setup cost for adapting to non-metals.	Feasible for specific non-contact applications if adapted with electrostatic clamping for polymers. More limited than other options due to material restrictions. High setup cost, requiring specialized electromagnetic chucks
Hydrostatic/Fluid [33]	– Shape-adaptive clamping – Even force distribution – Vibration dampening	– Complex system setup – Risk of contamination – Higher maintenance demands	Highly feasible for delicate IOL handling, providing uniform support around the complex geometry. High cost due to fluid management, seals, and the pressure regulation system.
Piezoelectric [34,35]	– Extreme precision – Gentle force application – Real-time control	– High cost and complexity – Limited holding strength	Low primary feasibility. High cost, as piezo-actuators and their associated high-voltage amplifiers are expensive.
Compliant [36]	– Adaptive and gentle holding – Simple customization	– Limited holding strength – Higher customization costs – Still an emerging technology	Highly suitable for handling and inspection of soft, curved lenses. Excellent for delicate, adaptive holding, though better suited to processes needing low to moderate holding strength. High initial engineering cost, low recurring cost.

5. Novel Clamping–Cooling System

After analyzing the advantages and challenges of available technologies, three key technologies were selected and integrated into the design of the novel clamping–cooling system: off-axis diamond turning for machining, a microchannel cooling system for thermal management, and vacuum clamping for workpiece fixation.

5.1. Structure Design and Material Selection

Figure 9 illustrates a simplified structure of the designed clamping–cooling system, combining a vacuum clamping mechanism with an embedded microchannel cooling network to ensure precise workpiece handling and effective thermal management during machining. This dual-function system addresses the specific demands of hydrophobic IOL machining, as discussed in Section 4, where strict control over mechanical stability and temperature is essential for maintaining optical quality and dimensional accuracy.

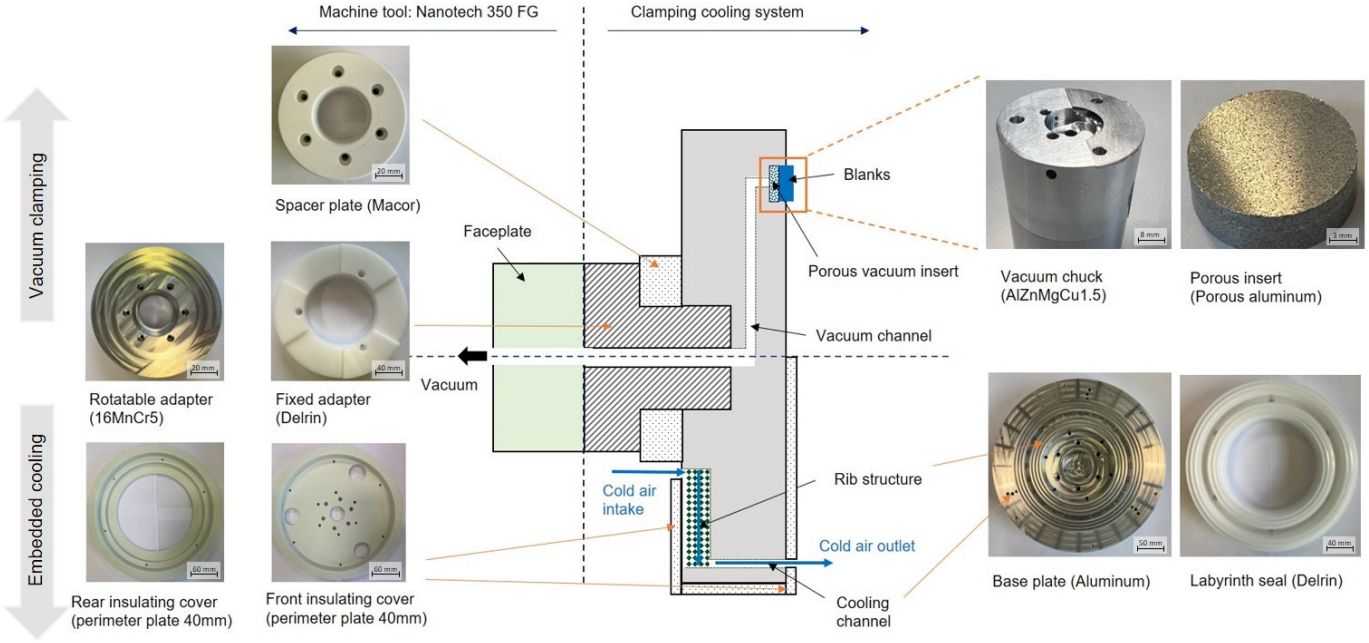

Figure 9. Schematic structure and corresponding parts of the clamping–cooling system.

In Figure 9 (upper side), the air evacuation process is shown, where air is drawn from the backside through vacuum channels, allowing for a uniform pressure distribution across the surface of the polymer blank via a porous vacuum insert that prevents localized pressure damage. To keep the blank temperature below the T_g, continuous cooling is applied through a ribbed structure: cold air is introduced at the rear and exits at the front (lower side of Figure 9).

Figure 10a provides a detailed view of the clamping–cooling system's structural design. The system begins with a rotatable adapter that securely connects to the machine spindle, providing a stable foundation and ensuring alignment of subsequent components. Outside the rotatable adapter is a fixed adapter. Together with the spacer plate directly after the rotatable adapter, they form a thermal insulation gap layer, effectively isolating the clamping–cooling system from heat transfer originating from the machine tool.

The design incorporates a concentric rib structure within the labyrinth seal and base plate, which fit together to create microchannels approximately 1 mm in width, distributed uniformly throughout the system. These microchannels are used to circulate cold air, providing consistent cooling across the system and helping maintain the low temperature essential for precision machining. During turning, the rotatable adapter, spacer plate, insulating cover, base plate, and vacuum chuck rotate in unison with the spindle. Meanwhile, the fixed adapter and labyrinth seal remain stationary and securely attached to the machine tool.

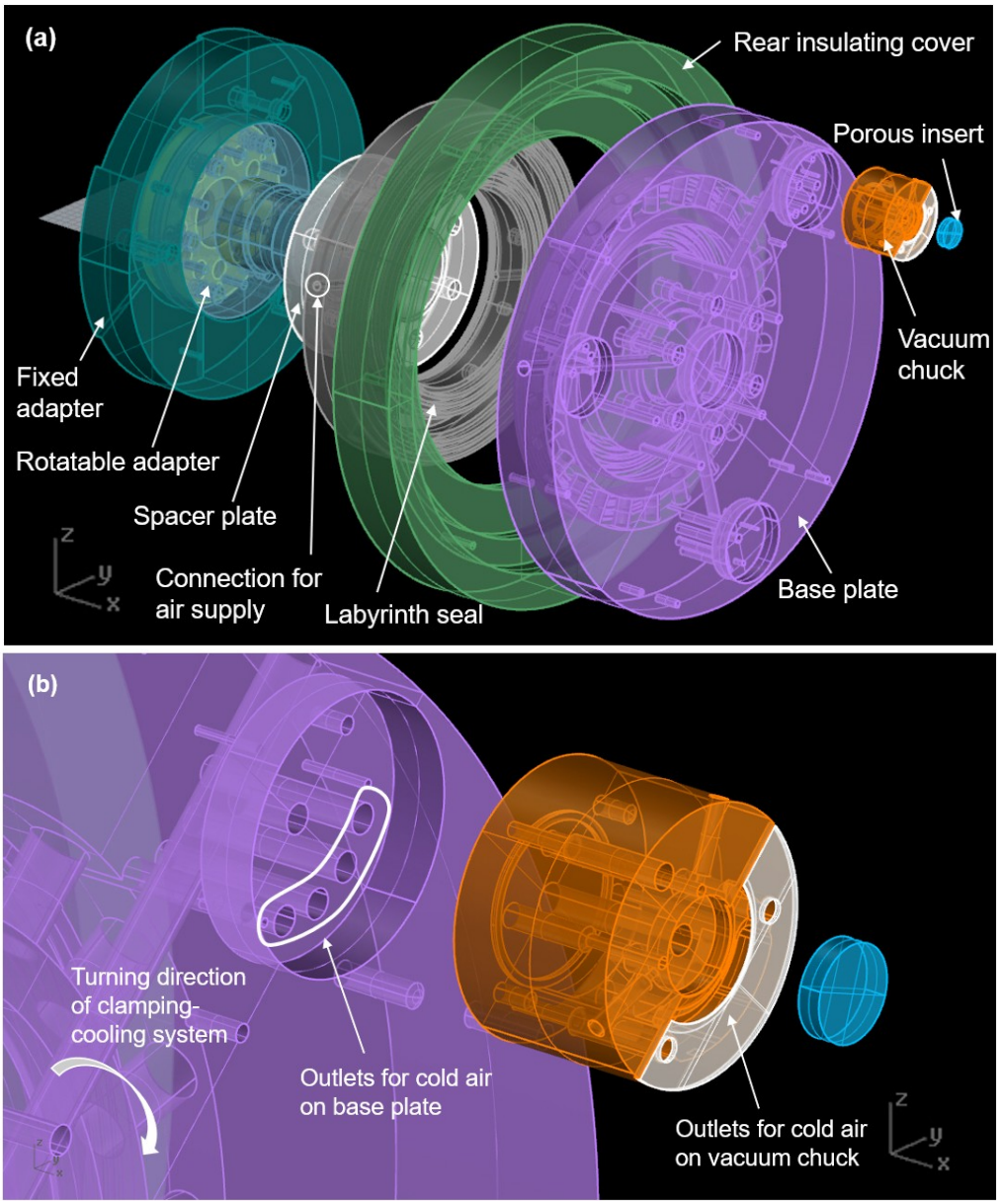

Figure 10. (**a**) 3D assembly of the clamping–cooling system. (**b**) Details of the vacuum chuck insert.

The three vacuum chucks are configured to match the lens positions, forming a rotationally symmetric layout with a 120° angle between each chuck. Each chuck is positioned 115 mm from the base plate's center. At the core of each vacuum chuck is a porous aluminum insert that securely holds the lens blanks. The cold air outlets are strategically positioned on the right side of the porous insert, as shown in Figure 10b. During clockwise rotation of the clamping–cooling system, the cold air flows smoothly over the lens blanks' surfaces, creating a veil that aids chip removal and provides targeted surface cooling; the trajectory of the exiting air is experimentally validated using visible smoke. This setup enables continuous temperature control and efficient chip movement, ensuring stable thermal conditions and preserving surface integrity throughout the machining process.

To address the need for thermal insulation in the clamping–cooling system, materials such as Delrin, Macor, and Perimeter plate were selected for the fixed adapter, spacer plate, labyrinth seal, and insulating cover. These materials exhibit low thermal conductivity (less than 1.5 W/(m·K)), effectively preventing unwanted heat transfer to maintain system stability. Conversely, materials for components requiring efficient heat dissipation, such

as the base plate, vacuum chuck, and porous insert, were selected for their high thermal conductivity properties, utilizing aluminum and AlZnMgCu1.5 alloys.

For the rotatable adapter, steel 16MnCr5 was chosen due to its balance of mechanical strength and moderate thermal conductivity, ensuring structural stability with reduced heat conduction. Importantly, thermal expansion was carefully considered in the design, and experiments confirmed that the clamping–cooling system operates reliably without jamming, even at temperatures below 0 °C. Related material properties are listed in Table 3.

Table 3. Material properties used in the clamping–cooling system.

Part	Material	Thermal Conductivity [W/(m·K)]	Thermal Expansion Coefficient α Around 20 °C [µm/(m·K)]
Rotatable adapter	16MnCr5	41	11.1–13.9
Fixed adapter	Polyoxymethylene	0.21–0.35	140–230
Spacer plate	Macor	1.46	9.3
Base plate	Aluminum	237	23
Labyrinth seal	Polyoxymethylene	0.21–0.35	140–230
Vacuum chuck	AlZnMgCu1.5	130–160	23.6
Porous insert	Porous aluminum	237	23
Insulating cover	Perimeter plate 40 mm	0.032–0.038	-

5.2. Performance Test

A performance test was conducted to evaluate the system's embedded cooling function, with the heat-exchange principle illustrated in Figure 11. The cooling supply for the system is a DYNEO DD-1000F Refrigeration Circulation Thermostat (Julabo GmbH, Seelbach, Germany), which uses a water-glycol solution (monoethylene glycol with anti-corrosion additives) as the cooling medium. This thermostat manages cooling medium temperatures from −50 °C to +200 °C, achieving a temperature stability of ±0.01 °C, and operates at ambient temperatures from +5 °C to +40 °C. Additionally, compressed air, initially at 22 °C and 3 bar pressure, serves as the cold air source. Cooling is achieved through the heat exchange circuit, where the compressed air flows through a customized plate heat exchanger, exchanging heat with the cooling medium.

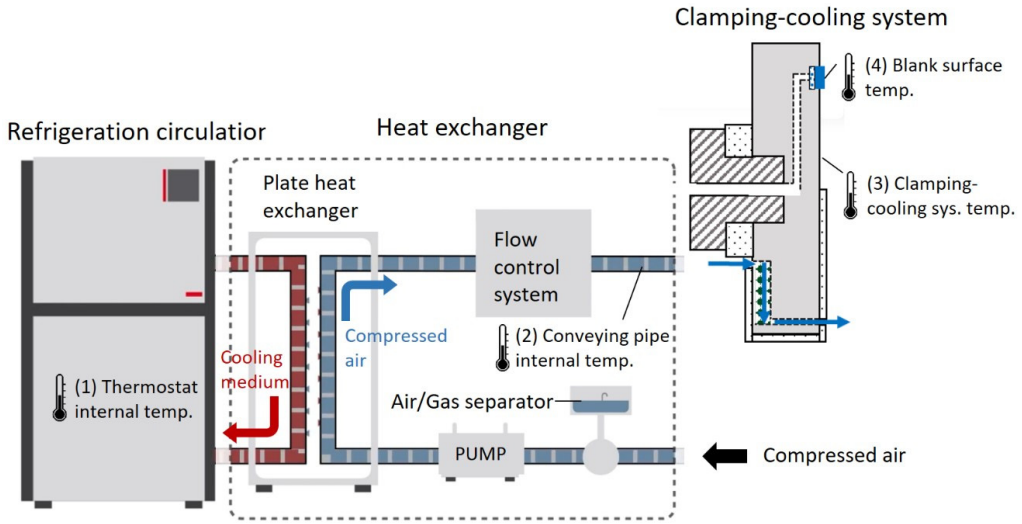

Figure 11. Principal layout of the supply system for compressed cold air and clamping–cooling system.

To validate the system's stationary cooling performance, a performance test was conducted using four temperature measurement points, as illustrated in Figure 11: (1) the thermostat's internal temperature, representing the cooling medium; (2) the internal

temperature of the conveying pipe, measured approximately 2 m before the clamping–cooling system; (3) the surface temperature of the clamping–cooling system; and (4) the surface temperature of the lens blank.

The (2) conveying pipe internal temperature acts as the in situ reference for feedback control, regulating the (1) thermostat internal temperature through embedded sensors. This feedback loop ensures precise temperature management by adjusting the thermostat settings based on real-time measurements from the conveying pipe, optimizing cooling performance. Temperatures at positions (3) and (4) are manually measured using thermocouples (Form C, Cu-CuNi; Conatex Mess-und Regeltechnik, Wendel, Germany) and read with a thermometer (GMH 3251; Conatex Mess-und Regeltechnik, Wendel, Germany).

A photograph of the experimental setup inside the machine tool for the cooling performance test is shown in Figure 12. In this setup, compressed cold air is evenly distributed by entering the clamping–cooling system via inlets on both the left and right sides. This symmetrical airflow arrangement ensures uniform cooling across the entire clamping–cooling system, enabling consistent thermal management throughout the machining process.

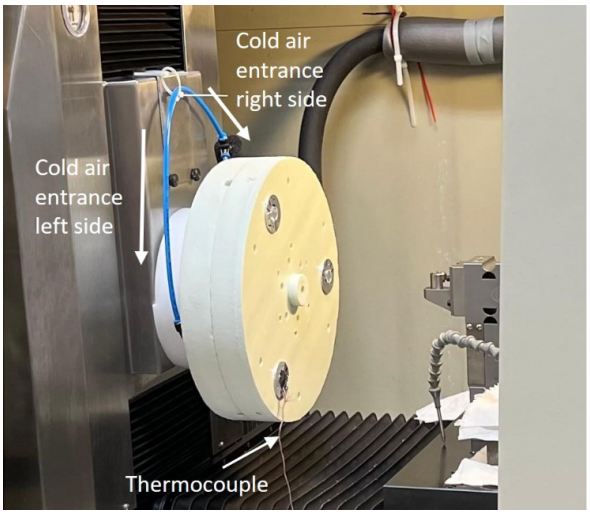

Figure 12. Experimental setup for the cooling performance test on the ultra-precision machine system.

Figure 13 illustrates the temperature development at the four measured positions when the target temperature, represented by position (2), is set to −10 °C. Each temperature measurement is recorded at one-minute intervals throughout the entire test. After approximately 30 min, the conveying pipe temperature reaches the set value of −10 °C, while the thermostat internal temperature at position (1) stabilizes around −14 °C due to thermal losses during transport. The lens blank surface temperature stabilizes at approximately 6 °C after 60 min. During this steady-state phase, the system demonstrated significant attenuation of thermal transients. Temperature at position (1) maintained extreme equilibrium, with fluctuations constrained to the sub-millikelvin range in accordance with the thermostat's control resolution. Although positions (2) and (3) exhibited slightly higher thermal fluctuations—attributed to ambient convection, the length of the conveying pipe, and measurement uncertainty—these disturbances were successfully dampened before they reached the workpiece. Consequently, despite being at the terminus of the thermal transfer chain and subject to ambient convective influences, the peak-to-peak temperature variation (ΔT_{pp}) at position (4) remained strictly within the sub-kelvin range at approximately 0.3 K, confirming the system's capacity for thermal stability.

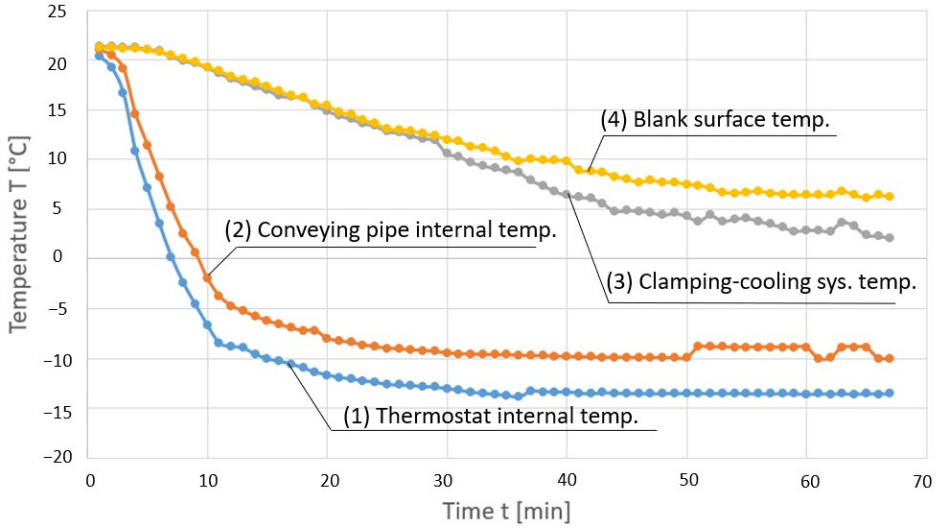

Figure 13. Temperature development in the supply system for cold air and the clamping–cooling system.

To evaluate the maximum cooling capacity of the secondary heat-exchange circuit, an additional experiment was conducted at a target temperature of −50 °C, with all other parameters held constant. After 60 min, the lowest temperature at position (2) stabilized at −20 °C, with the thermostat internal temperature reaching −24 °C. This temperature limitation is likely due to the pressure and volume constraints of the input compressed air. The surface temperature of the clamping–cooling system dropped below 0 °C after 60 min, enabling improved cooling of the hydrophobic blanks.

The significance of reaching these thermal levels is underscored by prior machinability studies [37] concerning the temperature-dependent ductility of hydrophobic acrylics. Under baseline parameters—comprising a turning speed of 100 rpm, a feed of 20 µm, and a depth of cut of 10 µm—the surface roughness Sa of SHi49 reached 560 nm at 20 °C. However, introducing a precooling step to 0 °C effectively reduced the Sa to 321.6 nm. When combined with optimized kinematic parameters (a turning speed of 1000 rpm, a feed of 2 µm, and a 10 µm depth of cut), the process yielded a nanometric surface finish (Sa = 5.9 nm). Consequently, the proposed system's capacity to reliably sustain sub-zero temperatures at the workpiece interface establishes the critical technical foundation for achieving nanoscale surface integrity within a scalable, off-axis production environment.

It should be noted that the temperatures measured in the non-rotating state are highly dependent on the measurement orientation; consequently, all recorded temperatures were obtained at a fixed angular position. While stationary testing enables a controlled evaluation of intrinsic cooling capacity, the thermal behavior during active machining is further influenced by the high-speed rotation of the clamping–cooling assembly. To estimate the influence of rotation on convective heat transfer, the flow regime surrounding the rotating assembly was characterized by the rotational Reynolds number (Re_ω), as defined in Equation (3):

$$Re_\omega = \frac{\rho \cdot \omega \cdot R_{offset}^{\,2}}{\mu} \quad (3)$$

where $\rho \approx 1.2$ kg/m^3 is the air density, $R_{offset} = 115$ mm is the offset radius, and $\mu \approx 1.8 \times 10^{-5}$ Pa·s is the dynamic viscosity of air. At a representative turning speed of n = 1000 rpm ($\omega \approx 105$ rad/s), the resulting Re_ω is around 9.2×10^4. In rotating fluid dynamics, the transition from laminar to turbulent flow on a rotating disk typically occurs at a critical Reynolds number (Re_c) of 2.4×10^5. Consequently, the system operates within the stable laminar regime during standard machining, where convective heat exchange with the ambient air is naturally limited.

Furthermore, any potential convective heat gain from the 20 °C ambient air is further suppressed by the integrated insulating cover. This cover serves as a critical thermal shield, preventing the development of a high-velocity boundary layer directly on the functional surfaces. Simultaneously, the rotation enhances the internal heat-extraction efficiency within the microchannels due to centrifugal forces, ensuring that the IOL substrate remains in its glassy state. This analysis suggests that the temperatures under actual machining conditions remain as stable as, or even lower than, those recorded during static characterization.

6. Summary

This study presents a novel clamping–cooling system specifically designed for the off-axis machining of hydrophobic IOLs, integrating advanced technologies for precise temperature regulation and mechanical stability. By combining vacuum clamping with embedded microchannel cooling, the system enhances both efficiency and accuracy in IOL production. Performance evaluations confirm its capability to maintain stable thermal conditions, minimizing deformation and preserving the optical integrity of the lenses.

The proposed system addresses the technological gap in off-axis machining with integrated in-process cooling. It tackles key challenges in IOL manufacturing, such as boosting production efficiency and ensuring precise thermal control when processing low-T_g hydrophobic polymers. Its modular design further ensures versatility, making it adaptable to a wide range of micro-optical component manufacturing processes.

Author Contributions: Conceptualization, W.W., O.R., K.R., T.E., A.B., and B.K.; methodology, W.W., O.R., and K.R.; validation, W.W.; formal analysis, W.W.; investigation, W.W.; resources, O.R., K.R., T.E., and B.K.; data curation, W.W.; writing—original draft preparation, W.W., and A.B.; writing—review and editing, W.W., O.R., K.R., T.E., A.B., and B.K.; visualization, W.W.; supervision, O.R., and B.K.; project administration, O.R., K.R., and T.E.; funding acquisition, O.R., K.R., T.E., and B.K. All authors have read and agreed to the published version of the manuscript.

Funding: This research and development project is funded by the German Federal Ministry of Education and Research (BMBF) within the "SME-innovative: Production Research" funding measure (funding number 02P21K521).

Data Availability Statement: The data presented in this study are available on request from the corresponding author.

Acknowledgments: This research and development project is managed by the Project Management Agency Karlsruhe (PTKA).

Conflicts of Interest: T.E. and A.B. are employees of AMIPLANT GmbH, which is an industrial partner in the BMBF-funded research project. The authors declare that this affiliation did not influence the objectivity of the research or the decision to publish the results. The remaining authors declare no conflicts of interest.

References

1. Li, C. Editorial for Special Issue on Ultra-Precision Machining of Difficult-to-Machine Materials. *Micromachines* **2025**, *16*, 1004. [CrossRef] [PubMed]
2. Ganesan, G.; Malayath, G.; Mote, R.G. A review of cutting tools for ultra-precision machining. *Mach. Sci. Technol.* **2022**, *26*, 923–976. [CrossRef]
3. Abdulkadir, L.N.; Abou-El-Hossein, K.; Jumare, A.I.; Odedeyi, P.B.; Liman, M.M.; Olaniyan, T.A. Ultra-precision diamond turning of optical silicon—A review. *Int. J. Adv. Manuf. Technol.* **2018**, *96*, 173–208. [CrossRef]
4. Mallick, P.S.; Pratap, A.; Patra, K. Review on cryogenic assisted micro-machining of soft polymer: An emphasis on molecular physics, chamber design, performance analysis and sustainability. *J. Manuf. Process.* **2022**, *80*, 930–957. [CrossRef]
5. Vacalebre, M.; Frison, R.; Corsaro, C.; Neri, F.; Santoro, A.; Conoci, S.; Anastasi, E.; Curatolo, M.C.; Fazio, E. Current State of the Art and Next Generation of Materials for a Customized IntraOcular Lens according to a Patient-Specific Eye Power. *Polymers* **2023**, *15*, 1590. [CrossRef]

6. Yu, N.; Fang, F.; Wu, B.; Zeng, L.; Cheng, Y. State of the art of intraocular lens manufacturing. *Int. J. Adv. Manuf. Technol.* **2018**, *98*, 1103–1130. [CrossRef]
7. Tommaso, R.; Mario, R.R.; Danilo, I.; Vito, R.; Luca, G.; Isabella, D.A.; Guido, R. Cataract surgery practice patterns worldwide: A survey. *BMJ Open Ophthalmol.* **2021**, *6*, e000464. [CrossRef]
8. Global Industry Analysts, Inc. *Intraocular Lenses—Global Strategic Business Report*; Global Industry Analysts Inc.: San Jose, CA, USA, 2024; p. 266.
9. Schrecker, J.; Schröder, S.; Langenbucher, A.; Seitz, B.; Eppig, T. Individually Customized IOL Versus Standard Spherical Aberration-Correcting IOL. *J. Refract. Surg.* **2019**, *35*, 565–574. [CrossRef]
10. Goel, B.; Singh, S.; Sarepaka, R.G.V. Precision Deterministic Machining of Polymethyl Methacrylate by Single-Point Diamond Turning. *Mater. Manuf. Process.* **2016**, *31*, 1917–1926. [CrossRef]
11. Mahajan, K.; Pawade, R.; Balasubramaniam, R. Experimental Study of Effect of Machining Parameters on PMMA in Diamond Turning. In *Advances in Manufacturing Processes; Lecture Notes in Mechanical Engineering*; Springer: Singapore, 2021; pp. 19–27.
12. Sarepaka, R.; Khatri, N.; Mishra, V. Optimization of Process Parameters to Achieve Nano Level Surface Quality on Polycarbonate. *Int. J. Comput. Appl.* **2012**, *48*, 39–44. [CrossRef]
13. Singh, H.; Vaishya, R.; Singh, K.; Mishra, V.; Sarepaka, R. Analysis of Surface Roughness and Waviness During Diamond Turning of Polycarbonate. *Int. J. Sci. Res.* **2012**, *2*, 268–270. [CrossRef]
14. Wang, W.; Riemer, O.; Rickens, K.; Eppig, T.; Karpuschewski, B. Off-Axis Fast-tool-servo diamond turning of customized intraocular lenses from hydrophobic acrylic polymer. In *Proceedings of the 24th EUSPEN International Conference and Exhibition, Dublin, Ireland, 10–14 June 2024*; EUSPEN: Bradfordshire, UK, 2024; pp. 221–222.
15. *ISO 11979-2:2024*; Ophthalmic Implants—Intraocular Lenses—Part 2: Optical Properties and Test Methods. International Organization for Standardization: Geneva, Switzerland, 2024.
16. *ISO 11979-3:2024*; Ophthalmic Implants—Intraocular Lenses—Part 3: Mechanical Properties and Test Methods. International Organization for Standardization: Geneva, Switzerland, 2024.
17. *ISO 25178-2:2021*; Geometrical Product Specifications—Surface Texture: Areal—Part 2: Terms, Definitions and Surface Texture Parameters. International Organization for Standardization: Geneva, Switzerland, 2021.
18. Miranda-Giraldo, M.; Serje, D.; Pacheco, J.; Bris, J. Burr formation and control for polymers micro-milling: A case study with vortex tube cooling. *Dyna* **2017**, *84*, 150–159. [CrossRef]
19. Yildiz, Y.; Nalbant, M. A review of cryogenic cooling in machining processes. *Int. J. Mach. Tools Manuf.* **2008**, *48*, 947–964. [CrossRef]
20. Rahim, E.A.; Ibrahim, M.R.; Rahim, A.A.; Aziz, S.; Mohid, Z. Experimental Investigation of Minimum Quantity Lubrication (MQL) as a Sustainable Cooling Technique. *Procedia CIRP* **2015**, *26*, 351–354. [CrossRef]
21. Du, K.; Calautit, J.; Wang, Z.; Wu, Y.; Liu, H. A review of the applications of phase change materials in cooling, heating and power generation in different temperature ranges. *Appl. Energy* **2018**, *220*, 242–273. [CrossRef]
22. Gilmore, N.; Timchenko, V.; Menictas, C. Microchannel cooling of concentrator photovoltaics: A review. *Renew. Sustain. Energy Rev.* **2018**, *90*, 1041–1059. [CrossRef]
23. Iyengar, M.; Garimella, S. Design and Optimization of Microchannel Cooling Systems. In *Proceedings of the Thermal and Thermomechanical Proceedings 10th Intersociety Conference on Phenomena in Electronics Systems, ITHERM, 30 May–2 June 2006*; IEEE: Piscataway, NJ, USA, 2006; pp. 54–62.
24. Baru, S.; Bhatia, S. A review on thermoelectric cooling technology and its applications. *IOP Conf. Ser. Mater. Sci. Eng.* **2020**, *912*, 042004. [CrossRef]
25. Kanbur, B.B.; Suping, S.; Duan, F. Design and optimization of conformal cooling channels for injection molding: A review. *Int. J. Adv. Manuf. Technol.* **2020**, *106*, 3253–3271. [CrossRef]
26. Kumar, A.; Vivekanand; Subudhi, S. Cooling and dehumidification using vortex tube. *Appl. Therm. Eng.* **2017**, *122*, 181–193. [CrossRef]
27. Cerchiari, G.; Yzombard, P.; Kellerbauer, A. Laser-Assisted Evaporative Cooling of Anions. *Phys. Rev. Lett.* **2019**, *123*, 103201. [CrossRef]
28. Williamson, R. Stresses Applied to Optical Components. In *Field Guide to Optical Fabrication*; SPIE: Bellingham, WA, USA, 2011. [CrossRef]
29. Zeng, L.; Liu, T.; Cheng, L.; Zhang, H.; Liu, K.; Liu, H.; Wang, Y. Liquid nitrogen assisted-ice clamping strategy to suppress milling force-induced deformation and residual stress release deformation in thin-walled cylindrical shells. *Thin-Walled Struct.* **2026**, *222*, 114488. [CrossRef]
30. Jantzen, S.; Stein, M.; Kniel, K.; Dietzel, A. Microclamping principles from the perspective of micrometrology—A review. *Precis. Eng.* **2017**, *50*, 538–550. [CrossRef]

31. Lei, X.-y.; Zhang, S.; Wang, S.; Zhang, J.-f.; Su, W.-h.; Zhang, L.-p.; An, C.; Wang, J.; Zhang, Q.-h.; Liu, M.-c.; et al. Influence of the arrangement of vacuum chuck holes on the transmittance wavefront of large-aperture KDP in single-point diamond turning. *Appl. Opt.* **2020**, *59*, 3619–3623. [CrossRef]
32. Baek, S.-W.; Yoon, K.-Y. Improving the Hybrid Electromagnetic Clamping System by Reducing the Leakage Flux and Enhancing the Effective Flux. *Energies* **2019**, *12*, 3762. [CrossRef]
33. Borden, Y.; Inman, D. A Hybrid Piezoelectric-Hydraulic Actuator Model and Prototype with Large Stroke and Force Parameters. In Proceedings of the ASME 2023 Conference on Smart Materials, Adaptive Structures and Intelligent Systems, Austin, TX, USA, 11–13 September 2023.
34. Li, Y.J.; Zhang, Q.; Wang, G.C. Research on Axis Piezoelectric Six-Axis Force/Torque Sensor Clamping Device. *Appl. Mech. Mater.* **2013**, *365–366*, 623–626. [CrossRef]
35. Gu, Y.; Xing, J. Dynamics analysis for the clamping mechanisms of a rotary inchworm piezoelectric motor. *J. Vibroeng.* **2016**, *18*, 2229–2239. [CrossRef]
36. Aoyama, T.; Kakinuma, Y. Development of Fixture Devices for Thin and Compliant Workpieces. *CIRP Ann.* **2005**, *54*, 325–328. [CrossRef]
37. Wang, W.; Riemer, O.; Rickens, K.; Eppig, T.; Karpuschewski, B. Machinability of hydrophobic acrylic polymer for customized intraocular lenses. In Proceedings of the 9th International Conference on Nanomanufacturing (nanoMan2024), Singapore, 1–4 December 2024; pp. 100–103.

Disclaimer/Publisher's Note: The statements, opinions and data contained in all publications are solely those of the individual author(s) and contributor(s) and not of MDPI and/or the editor(s). MDPI and/or the editor(s) disclaim responsibility for any injury to people or property resulting from any ideas, methods, instructions or products referred to in the content.